Journal of Nuclear Materials 479 (2016) 162–166

Contents lists available at ScienceDirect

Journal of Nuclear Materials

journal homepage: www.elsevier.com/locate/jnucmat

Preparation of low-temperature sintered UO_2 nanomaterials by radiolytic reduction of ammonium uranyl tricarbonate

Yongming Wang, Qingde Chen*, Xinghai Shen**

Beijing National Laboratory for Molecular Sciences, Fundamental Science on Radiochemistry and Radiation Chemistry Laboratory, College of Chemistry and Molecular Engineering, Peking University, Beijing 100871, PR China

HIGHLIGHTS

- UO_2 nanoparticles were synthesized by the radiolytic reduction of $(NH_4)_4UO_2(CO_3)_3$ with high efficiency.
- The as-prepared UO_2 nanoparticles were stable in the irradiated mother solution exposed to air atmosphere.
- UO_2powders could be sintered at 450–600 °C in vacuum, much lower than that in traditional process.

ARTICLE INFO

Article history:
Received 29 March 2016
Received in revised form
1 July 2016
Accepted 4 July 2016
Available online 7 July 2016

Keywords:
UO_2
Nanoparticles
Ammonium uranyl tricarbonate (AUC)
Nuclear fuels
γ-irradiation

ABSTRACT

UO_2 nanoparticles were successfully obtained from ammonium uranyl tricarbonate with high efficiency by γ-irradiation. More importantly, the as-prepared nanoparticles were stable in the irradiated mother solution exposed to air atmosphere. The purified UO_2 powders could be sintered at 450–600 °C, much lower than the reported values (above 1700 °C) of bulk UO_2. These advantages made this method promising in the production of UO_2 nuclear fuels.

1. Introduction

In the past half-century, many methods were developed to improve the performance of UO_2, one of the most important nuclear fuels. However, there are still several intractable problems, especially the sintering temperature as high as 1700 °C or more [1,2]. In the literature, two- and three-step sintering processes at 1100–1500 °C favored the production of high density UO_2 fuel pellets [3,4]. Therefore, it is fascinating to explore novel methods to prepare UO_2 which can be sintered at relatively low temperature.

With the development of nanoscience and nanotechnology, some new techniques were employed to prepare uranium oxide nanoparticles and nanostructures. Wu et al. [5] first prepared nearly monodispersed UO_2 nanocrystals using organic thermal decomposition method and proposed the application of UO_2 nanocrystals in the fields of nuclear fuel fabrication and catalysis. This inspired an enthusiasm greatly in the preparation of uranium oxide nanoparticles and nanostructures. So far, quasi-spherical UO_2 nanoparticles [5–9], flower-like U_3O_8 nanostructures [10], U_3O_8 nanorods [6,9], U_3O_8 nanotubes [11], and hierarchical uranium oxides nano-/microspheres [10,11] were obtained by thermochemical and electrochemical methods. Furthermore, it was verified that some nano-sized uranium oxide particles exhibited a much better catalytic performance than their bulk materials [6,10,12,13].

Among the numerous methods of preparing nanoparticles, ionizing irradiation (such as γ-irradiation, electron beam irradiation and so on) is powerful, since it can conveniently produce a series of species with tunable redox potentials to reduce metal ions in a wide temperature range [14,15]. In the preparation of uranium-containing nanoparticles, this method also played an important role [16–19]. Roth and coworkers [16] first synthesized UO_2 nanoparticles *via* ionizing irradiation. Nenoff et al. [17] also

* Corresponding author.
** Corresponding author.
E-mail addresses: qdchen@pku.edu.cn (Q. Chen), xshen@pku.edu.cn (X. Shen).

http://dx.doi.org/10.1016/j.jnucmat.2016.07.003
0022-3115/

obtained UO_2 nanoparticles by a similar method, and directly observed their sintering in the range of 500–600 °C, much lower than the reported values of bulk UO_2 (above 1700 °C) on a transmission electron microscopy (TEM) with an in situ heating stage. However, the subsequent work of Rath and collaborators [18] indicated that most of the UO_2 nanoparticles prepared by radiolytic method could be oxidized in air atmosphere and dissolved in the solution again in a short time (*e.g.*, 8 h). This made it much difficult for the application of radiolytic method in fabricating nuclear fuels. To the best of our knowledge, in the method, almost all UO_2 nanoparticles were synthesized from $UO_2(NO_3)_2$ in acidic solution. Because bulk UO_2 could be dissolved in HNO_3 slowly but not in ammonia, alkali and carbonate solutions [20–22], it worth exploring in basic condition. In addition, for their existing form of sol in the irradiated mother liquor, the as-prepared UO_2 nanoparticles have a large surface area and a high surface energy, which may make them much active in their reaction with oxygen. From this point of view, a suitable aggregation may improve the stability of UO_2 nanoparticles.

In the last decade, we tried our best to control the radiolytic syntheses of nanoparticles and nanostructures. Mesoporous $BaSO_4$ microspheres [23], octahedron Cu_2O nanocrystals [24], solid and hollow Cu_2O nanocubes [25], and prismatic $PbSO_4$ microcrystals [26] were successfully synthesized. In the present work, stable UO_2 nanoparticles are prepared by the radiolytic reduction of alkaline $(NH_4)_4UO_2(CO_3)_3$, which is a very important material in the production of UO_2 nuclear fuels industry. Then, the sintering properties are further investigated.

2. Experimental

$UO_2(NO_3)_2{\cdot}6H_2O$ (G.R., Chemapol, Prague Czechoslovakia), $HCOONH_4$, NH_4HCO_3, and Na_2CO_3 were of A.R. grade and were used without further purification. Ultrapure water was used throughout the experiments.

Ammonium uranyl tricarbonate (AUC) crystal was prepared according to Ref. [27]. $UO_2(NO_3)_2{\cdot}6H_2O$ was heated in a muffle furnace at 350 °C for 3 h, then an orange-yellow powder was obtained. The saturated NH_4HCO_3 solution was added slowly into a flask containing the orange-yellow powder with constant stirring at 60 °C until a yellow and clear solution was formed. When the solution cooled to room temperature, yellow AUC was precipitated from the solution. The result of elemental analysis was identical with the theoretical value. Elemental analysis: calcd (%) for $(NH_4)_4[UO_2(CO_3)_3]$ (M_r = 522.21): C 6.90, H 3.09, N 10.73; found (%): C 6.87, H 3.09, N 10.70.

A solution containing 20 mmol L^{-1} AUC, 100 mmol L^{-1} $HCOONH_4$, and 60 mmol L^{-1} Na_2CO_3 was prepared, where Na_2CO_3 was used as stabilizer. After bubbling with ultrapure N_2 for 20 min, the solution at room temperature was irradiated in the Gamma Irradiation Facility of Peking University using ^{60}Co γ-ray source for a fixed time at a special location whose dose rate was determined by a ferrous sulfate dosimeter. The pH values of the solution before and after irradiation were measured to be 9.26 and 9.38, respectively. After irradiation, black precipitates were obtained. The deposition efficiency (E_d) and the apparent G value (G_{app})[28] were calculated as follows:

$$E_d = \frac{c_0 - c_{end}}{c_0} \times 100\% \quad (1)$$

$$G_{app} = 9.647 \times 10^6 \times \frac{c_0 - c_{end}}{D \cdot \rho} \quad (2)$$

where c_0 and c_{end} (mol·L^{-1}) are the concentrations of uranium in the mother solution before and after irradiation, D (Gy) is the absorbed dose, and ρ (g·cm^{-3}) is the density of solution.

The black precipitates were collected by low-speed centrifugation immediately and thoroughly washed by water, dried in a vacuum oven overnight at room temperature, and then black powders were achieved. The well washed powders were dispersed in water, and were dropped onto a carbon-coated copper grid. After the solvent was evaporated at room temperature, transmission electron microscopy (TEM) images were carried out on a FEI Tacnai G2 T20 microscope operated at 200 kV. Scanning electron spectroscopy (SEM) images were obtained by a FEI nanoSEM 430 scanning electron microscope operated at 10 kV. In addition, after the dispersed sample was deposited on a piece of glass, the powder X-ray diffraction (XRD) patterns were recorded on a Rigaku Dmax-2000 diffractometer with Cu Kα radiation (λ = 0.15418 nm) and the average size of nanoparticles were calculated by Scherrer's formula based on the most strength (111) diffraction peak. DSC was measured on Q600 SDT TGA-DSC-DTA analyzer with temperature-programming 10 K/min in N_2 atmosphere. The concentration of U(VI) in the solution was analyzed on an Inductively Coupled Plasma-Atomic Emission Spectrometer (ICP-AES, Leeman, USA). Thermal treatment experiments in vacuum were conducted on a tube furnace for 100 min.

3. Results and discussion

Fig. 1 exhibits the effect of the absorbed dose on the deposition efficiency of uranium and the apparent G value at a fixed dose rates of 160 Gy min^{-1}. With an increase in the absorbed dose, the deposition efficiency increases obviously, while the apparent G value decreases due to the decrease of uranium concentration. At an absorbed dose of 150 kGy, the deposition efficiency reaches 99.7%. Furthermore, *via* fixing the absorbed dose at 150 kGy and altering dose rate in the range of 20–267 Gy min^{-1}, it was found that the deposition efficiency was not affected significantly. Therefore, the absorbed dose of 150 kGy and the dose rate of 160 Gy min^{-1} were applied in the following investigation.

Fig. 2A shows the SEM image of the as-prepared precipitate, it can be seen that the precipitate consists of quasi-spherical nanoparticles with a diameter of 50–200 nm. The corresponding TEM image (Fig. 2B) shows that the margin of the particles is quite coarse. So we speculate that they are composed of some smaller nanoparticles. In the related XRD pattern (curve a, Fig. 3), besides a broad peak at *ca.* 20° coming from the scattering of glass, four broaden (111), (200), (220) and (311) diffraction peaks

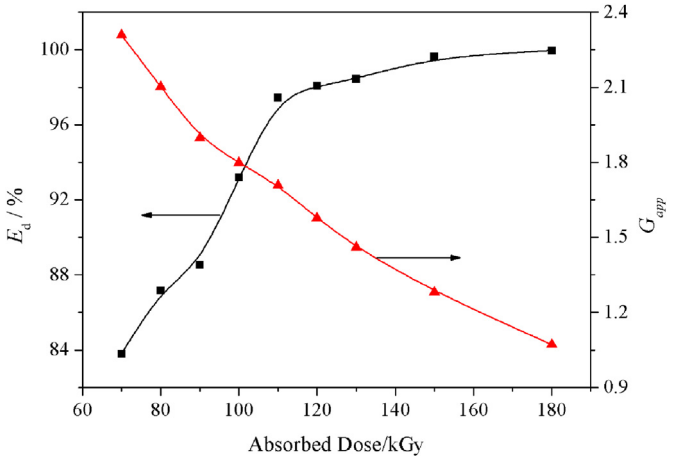

Fig. 1. Effect of absorbed dose on the deposition efficiency of uranium and the apparent G values. Dose rate: 160 Gy min^{-1}.

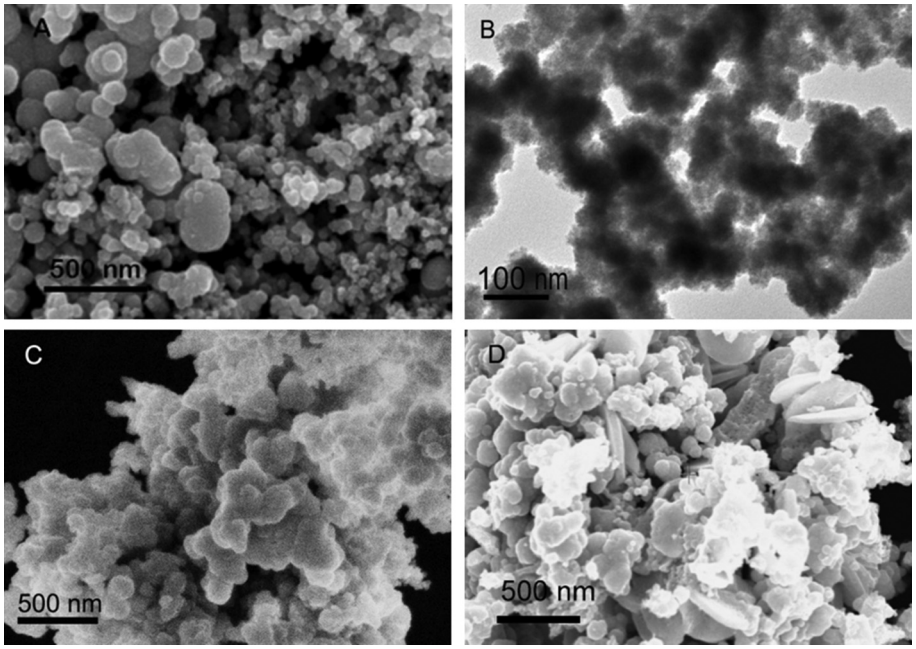

Fig. 2. SEM (A, C and D) and TEM (B) images of the products before (A and B) and after (C and D) thermal treatment in vacuum. Thermal treatment temperature: (C) 450 °C, (D) 600 °C.

corresponding to cubic phase UO_2 (JCPDS file No. 41-1422) are observed. This indicates the formation of cubic phase UO_2. Moreover, based on the (111) diffraction peak, the average size is estimated to be about 5 nm by using Scherrer's formula, confirming our speculation based on the TEM image.

In our experiment, when the aqueous solution was irradiated by γ-rays, the water molecules absorbed most of the irradiation energy and generated many reactive species, such as hydrated electrons (e^-_{aq}), ·H and ·OH and so on (Eq. (3))[29].

$$H_2O \xrightarrow{\text{irradiated}} e^-_{aq},\ \cdot H,\ \cdot OH, H_2, H_2O_2, H_3O^+ \cdots\cdots \quad (3)$$

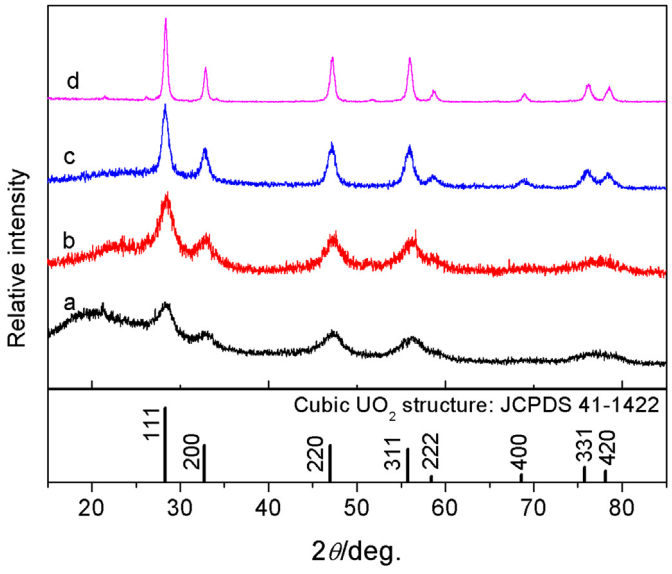

Fig. 3. XRD patterns of the products before (a) and after (b–d) thermal treatment in vacuum. Thermal treatment temperature: (a) as-prepared, (b) 400 °C, (c) 450 °C, (d) 600 °C.

Then the oxidative ·OH and the reductive ·H were eliminated by $HCOO^-$ with the rate constants of 3.2×10^9 and 2.1×10^8 L mol^{-1} s^{-1}, respectively (Eq. (4))[29].

$$HCOO^- + \cdot OH(\cdot H) \rightarrow \cdot CO_2^- + H_2O(H_2) \quad (4)$$

The reducing species, *e.g.*, e^-_{aq} and possible $\cdot CO_2^-$, reduced the precursors $UO_2(CO_3)_3^{4-}$ ions to U(IV) ions. Whereafter, $U(OH)_4$ was generated in the basic aqueous solution, which was transformed to UO_2 *via* dehydration (Eq. (5)).

$$UO_2(CO_3)_3^{4-} \xrightarrow{e^-_{aq}} U(IV) \xrightarrow{OH^-} U(OH)_4 \xrightarrow{-H_2O} UO_2(s) \quad (5)$$

It may be the low solubility of $U(OH)_4$ ($pK_{sp} = 52$) [21] that leads to its quick precipitation, the formation of nanoparticles and the follow-up aggregates. Besides, part of nanoparticles exists in the form of sol. The sol could be destroyed by salts (*i.e.*, Na_2CO_3 and $HCOONH_4$), favoring the aggregation of nanoparticles.

Fig. 4 is the DSC spectrum of the as-prepared UO_2 powders. As seen, there is a weak peak at *ca.* 440 °C, which may correspond to the melting of some UO_2 nanoparticles. With respect to the appearance of the broad peak, it may suggest the existence of a few impurities (such as U(IV) hydroxide). Thus, three thermal treatment experiments in vacuum were performed at 400, 450, and 600 °C, respectively. The XRD analyses of the heat-treated products (curves b, c and d, Fig. 3) indicate that they are all cubic phase UO_2 (JCPDS file no. 41-1422). Besides, the XRD pattern of the product treated at 400 °C (curve c, Fig. 3) does not change obviously as compared with that of the product directly synthesized by γ-rays (curve a, Fig. 3). Moreover, the average size of nanoparticles is estimated to be 5 nm, close to that before thermal treatment. When the heat-treatment temperature increases to 450 °C, the diffraction peaks become sharp, and there appear (222), (400), (331), and (420) diffraction peaks corresponding to cubic phase UO_2 (curve c, Fig. 3), and the average size of nanoparticles increases to *ca.* 13 nm. As the heat-treatment temperature increases to 600 °C, the peaks in the XRD spectrum of the product (curve d, Fig. 3) are further sharpened, and

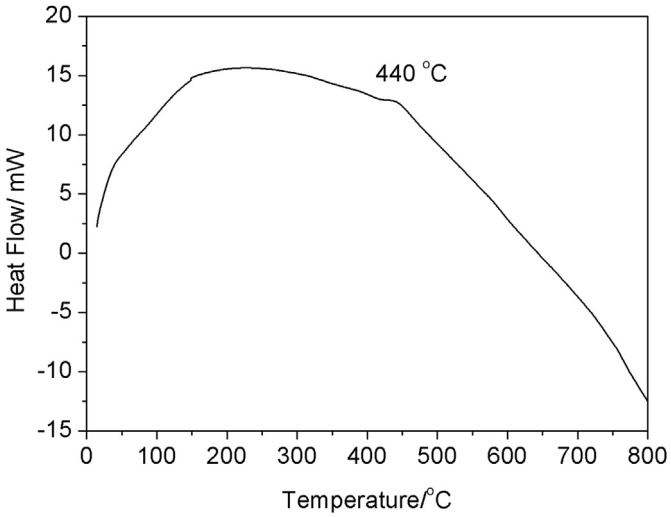

Fig. 4. DSC curve of the UO_2 powder synthesized by γ-irradiation in N_2 atmosphere. Absorbed dose: 150 kGy, dose rate: 160 Gy min^{-1}.

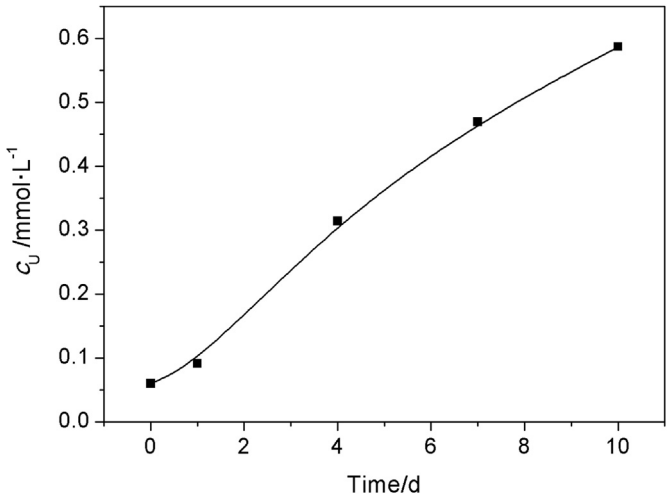

Fig. 5. Effect of time on the concentration of uranium in the irradiated mother solution exposed to air atmosphere. Absorbed dose: 150 kGy, dose rate: 160 Gy min^{-1}.

the average size of nanoparticles increases to *ca.* 35 nm. This represents that there happens fusion among nanoparticles at the temperature range of 450–600 °C.

A more intuitionistic proof comes from the related SEM images (Fig. 2C and D). At the heat-treatment temperature of 450 °C, the SEM image (Fig. 2C) shows that the product consists of nanoaggregates, and a lot of them have a tendency to form a flat structure with an irregular margin, which is obviously different from that of the product directly synthesized by γ-rays (Fig. 2A). This illustrates that a local sintering takes place in the process of thermal treatment. Furthermore, in the SEM image of the product after sintering at 600 °C (Fig. 2D), there appears a lot of disk-like nanoparticles with smooth surface as well as some spherical and irregular nanostructures, indicating the occurrence of an effective sintering among nanoparticles. If this method used in the production of UO_2 pellets, the energy consumption will be reduced greatly and the requirements to apparatuses will decrease for the relatively low sintering temperature.

Although the as-prepared UO_2 nanoparticles could be sintered at a relatively low temperature, this method could not be applied to prepare UO_2 nuclear fuels if the UO_2 nanoparticles were not stable. Therefore, a stability test was performed. After irradiation, the mixture of UO_2 precipitate and the mother solution was directly exposed to air atmosphere for several days. Fig. 5 shows the effect of exposure time on the concentration of uranium in the mother solution. After a day, only 3.15×10^{-2} mmol L^{-1} (*i.e.*, 0.2%) uranium was dissolved. After 10 days, the concentration of uranium in the solution was only increased by 2.6% (*i.e.*, 0.527 mmol L^{-1}), and the precipitate was still black. This indicates that the as-prepared UO_2 nanoparticles are much stable, favoring the application of radiolytic method in the preparation of UO_2 nuclear fuels.

With respect to the improvement of stability, there may be two reasons. Firstly, in air atmosphere, UO_2 is more stable in alkaline solution than in HNO_3 solution [20–22]. Secondly, the aggregation reduces the surface area and surface energy of UO_2 nanoparticles, leading to the decrease of their reactivity with oxygen.

4. Conclusion

UO_2 nanoparticles were successfully obtained from $(NH_4)_4UO_2(CO_3)_3$ with high efficiency by γ-irradiation. More importantly, the as-prepared nanoparticles were stable in the irradiated mother solution exposed to air atmosphere. The purified UO_2 powders could be sintered at 450–600 °C, much lower than 1700 °C, the temperature for preparing ceramic UO_2 nuclear fuels in traditional process. Based on the obvious advantages (*e.g.*, stable UO_2 nanoparticles, relatively low sintering temperature, high deposition efficiency), it is believed that this method is promising in the fabrication of UO_2 nuclear fuels.

Acknowledgements

This work was supported by National Natural Science Foundation of China (Grant No. 91226112) and the specialized research fund for the Doctored Program of Higher Education of China (Grant No. 20110001120121). Sincere thank are due to Mr. Deliang Sun and Mr. Jiuqiang Li for assistance in the γ-irradiation experiments.

References

[1] D. Sutarya, B. Kusumoputro, Identification of industrial furnace temperature for sintering process in nuclear fuel fabrication using NARX neural networks, Sci. Technol. Nucl. Install. (2014) 1–8, http://dx.doi.org/10.1155/2014/854569.
[2] C. Zhu, D. He, G. Wu, Y. Liao, Z. Yang, J. Liu, B. Hu, The industrial practice of AUC process for producing ceramic UO_2 in China, China Nucl. Sci. Technol. Rep. (2000). CNIC 01478, SINRE 00091.
[3] B. Ayaz, A.N. Bilge, The possible usage of ex-ADU uranium dioxide fuel pellets with low-temperature sintering, J. Nucl. Mater 280 (2000) 45–50, http://dx.doi.org/10.1016/s0022-3115(00)00033-7.
[4] Y. Harada, UO_2 sintering in controlled oxygen atmospheres of three-stage process, J. Nucl. Mater 245 (1997) 217–223, http://dx.doi.org/10.1016/s0022-3115(96)00755-6.
[5] H.M. Wu, Y.A. Yang, Y.C. Cao, Synthesis of colloidal uranium-dioxide nanocrystals, J. Am. Chem. Soc. 128 (2006) 16522–16523, http://dx.doi.org/10.1021/ja067940p.
[6] Q. Wang, G. Li, S. Xu, J. Li, J. Chen, Synthesis of uranium oxide nanoparticles and their catalytic performance for benzyl alcohol conversion to benzaldehyde, J. Mater. Chem. 18 (2008) 1146–1152, http://dx.doi.org/10.1039/b716990f.
[7] D. Hudry, C. Apostolidis, O. Walter, T. Gouder, E. Courtois, C. Kubel, D. Meyer, Non-aqueous synthesis of isotropic and anisotropic actinide oxide nanocrystals, Chem. -Eur. J. 18 (2012) 8283–8287, http://dx.doi.org/10.1002/chem.201200513.
[8] D. Hudry, C. Apostolidis, O. Walter, T. Gouder, E. Courtois, C. Kubel, D. Meyer, Controlled synthesis of thorium and uranium oxide nanocrystals, Chem. -Eur. J. 19 (2013) 5297–5305, http://dx.doi.org/10.1002/chem.201203888.
[9] R. Zhao, L. Wang, Z. Gu, L. Yuan, C. Xiao, Y. Zhao, Z. Chai, W. Shi, A facile additive-free method for tunable fabrication of UO_2 and U_3O_8 nanoparticles in aqueous solution, CrystEngComm 16 (2014) 2645–2651, http://dx.doi.org/10.1039/c3ce42140f.
[10] M. Pradhan, S. Sarkar, A.K. Sinha, M. Basu, T. Pal, Morphology controlled uranium oxide hydroxide hydrate for catalysis, luminescence and SERS

studies, CrystEngComm 13 (2011) 2878–2889, http://dx.doi.org/10.1039/c0ce00666a.
[11] L. Wang, R. Zhao, C.Z. Wang, L.Y. Yuan, Z.J. Gu, C.L. Xiao, S.A. Wang, X.W. Wang, Y.L. Zhao, Z.F. Chai, W.Q. Shi, Template-free synthesis and mechanistic study of porous three-dimensional hierarchical uranium-containing and uranium oxide microspheres, Chem. -Eur. J. 20 (2014) 12655–12662, http://dx.doi.org/10.1002/chem.201403724.
[12] G.J. Hutchings, C.S. Heneghan, I.D. Hudson, S.H. Taylor, Uranium-oxide-based catalysts for the destruction of volatile chloro-organic compounds, Nature 384 (1996) 341–343, http://dx.doi.org/10.1038/384341a0.
[13] H. Madhavaram, H. Idriss, Evidence of furan formation from ethanol over β-UO_3, J. Catal. 184 (1999) 553–556, http://dx.doi.org/10.1006/jcat.1999.2453.
[14] J. Belloni, Nucleation, growth and properties of nanoclusters studied by radiation chemistry - application to catalysis, Catal. Today 113 (2006) 141–156, http://dx.doi.org/10.1016/j.cattod.2005.11.082.
[15] Q.D. Chen, X.H. Shen, H.C. Gao, Radiolytic syntheses of nanoparticles in supramolecular assemblies, Adv. Colloid Interface Sci. 159 (2010) 32–44, http://dx.doi.org/10.1016/j.cis.2010.05.002.
[16] O. Roth, H. Hasselberg, M. Jonsson, Radiation chemical synthesis and characterization of UO_2 nanoparticles, J. Nucl. Mater 383 (2009) 231–236, http://dx.doi.org/10.1016/j.jnucmat.2008.09.026.
[17] T.M. Nenoff, B.W. Jacobs, D.B. Robinson, P.P. Provencio, J. Huang, S. Ferreira, D.J. Hanson, Synthesis and low temperature in situ sintering of uranium oxide nanoparticles, Chem. Mater 23 (2011) 5185–5190, http://dx.doi.org/10.1021/cm2020669.
[18] M.C. Rath, D.B. Naik, S.K. Sarkar, Reversible growth of UO_2 nanoparticles in aqueous solutions through 7 MeV electron beam irradiation, J. Nucl. Mater 438 (2013) 26–31, http://dx.doi.org/10.1016/j.jnucmat.2013.02.005.
[19] T.M. Nenoff, S.R. Ferriera, J. Huang, D.J. Hanson, Formation of uranium based nanoparticles via γ-irradiation, J. Nucl. Mater 442 (2013) 162–167, http://dx.doi.org/10.1016/j.jnucmat.2013.08.027.
[20] I. Grenthe, D. Ferri, F. Salvatore, G. Riccio, Studies on metal carbonate equilibria. Part 10. A solubility study of the complex formation in the uranium(VI)-water-carbon dioxide(g) system at 25 °C, J. Chem. Soc. Dalton Trans. (1984) 2439–2443, http://dx.doi.org/10.1039/DT9840002439.
[21] Y.D. Chen, W.J. Wang, Z.L. Wang, Z.M. Zhou, Chemistry of Nuclear Fuel, Atomic Energy Press, Beijing, 1985.
[22] X.D. Bai, Chemistry of Nuclear Materials, Chemical Industry Press, Beijing, 2007.
[23] Q.D. Chen, X.H. Shen, Formation of mesoporous $BaSO_4$ microspheres with a larger pore size via ostwald ripening at room temperature, Cryst. Growth Des. 10 (2010) 3838–3842, http://dx.doi.org/10.1021/cg100307r.
[24] P. He, X.H. Shen, H.C. Gao, Size-controlled preparation of Cu_2O octahedron nanocrystals and studies on their optical absorption, J. Colloid Interface Sci. 284 (2005) 510–515, http://dx.doi.org/10.1016/j.jcis.2004.10.060.
[25] Q.D. Chen, X.H. Shen, H.C. Gao, Formation of solid and hollow cuprous oxide nanocubes in water-in-oil microemulsions controlled by the yield of hydrated electrons, J. Colloid Interface Sci. 312 (2007) 272–278, http://dx.doi.org/10.1016/j.jcis.2007.03.036.
[26] J. Zhou, H.K. Zhao, J.F. Shi, Q.D. Chen, X.H. Shen, Radiolytic synthesis of prismatical $PbSO_4$ microcrystals, Radiat. Phys. Chem. 97 (2014) 366–369, http://dx.doi.org/10.1016/j.radphyschem.2013.07.027.
[27] K. Wu, The solubility of ammonium uranyl tricarbonate (AUC), At. Energy Sci. Technol. 3 (1961) 148–156.
[28] J.L. Wu, S.C. Qi, Radiation Chemistry, Atomic Energy Press, Beijing, 1993.
[29] G.V. Buxton, C.L. Greenstock, W.P. Helman, A.B. Ross, Rate constants for reactions of hydrated electrons, hydrogen atoms and hydroxyl radicals in aqueous solution, J. Phys. Chem. Ref. Data 17 (1988) 531–886.